University of Groningen

Identifying the Nature of Charge Recombination in Organic Solar Cells from Charge-Transfer State Electroluminescence

Wetzelaer, Gert-Jan A. H.; Kuik, Martijn; Blom, Paul W. M.

FULL PAPER

Identifying the Nature of Charge Recombination in Organic Solar Cells from Charge-Transfer State Electroluminescence

Gert-Jan A. H. Wetzelaer, Martijn Kuik, and Paul W. M. Blom*

Charge-transfer (CT) state electroluminescence is investigated in several polymer:fullerene bulk heterojunction solar cells. The ideality factor of the electroluminescence reveals that the CT emission in polymer:fullerene solar cells originates from free-carrier bimolecular recombination at the donor-acceptor interface, rather than a charge-trap-mediated process. The fingerprint of the presence of nonradiative trap-assisted recombination, a voltage-dependent CT electroluminescence quantum efficiency, is only observed for the P3HT:PCBM system, which is explained by a reduction of the competing bimolecular recombination rate. These results are in agreement with measurements of the illumination-intensity dependence of the open-circuit voltage.

1. Introduction

The performance of organic solar cells has shown continuous increase in recent years, reaching power-conversion efficiencies up to 10%.[1,2] However, further improvement is necessary to compete with inorganic technology, requiring a thorough fundamental understanding of the loss mechanisms taking place. One of the main limiting factors in the power-conversion process in organic photovoltaics is the recombination of photogenerated charges. Recombination in low-mobility materials is usually described by bimolecular recombination of the Langevin type,[3–5] determined by diffusion of free carriers towards each other in their mutual Coulomb field. Recently, it has been demonstrated that trapped charges may also take part in the recombination process.[6–11] In that case, a charge carrier is first trapped on an isolated site within the energy band gap, followed by recombination with a mobile carrier of opposite sign, as implied by Shockley-Read-Hall (SRH) statistics.[12,13] The presence of SRH recombination has been identified in all-polymer solar cells,[7] organic light-emitting diodes (OLEDs)[8–10] and

G. A. H. Wetzelaer, M. Kuik, Prof. P. W. M. Blom
Molecular Electronics
Zernike Institute for Advanced Materials
University of Groningen
Nijenborgh 4, 9747 AG Groningen, The Netherlands
E-mail: p.w.m.blom@rug.nl
G. A. H. Wetzelaer
Dutch Polymer Institute
PO Box 902, 5600 AX Eindhoven, The Netherlands
Prof. P. W. M. Blom
TNO/Holst Centre
High Tech Campus 31, 5605 KN Eindhoven, The Netherlands

polymer:fullerene solar cells with intentionally added impurities.[6,11]

In addition to inducing a second recombination channel, the presence of traps also limits charge transport in organic semiconductors. It has been observed that electron transport in organic materials is frequently hindered by electron traps, while hole transport generally shows trap-free behavior.[14,15] As a result, SRH-type recombination *via* electron traps is naturally present in organic light-emitting diodes made from a single conjugated material.[8] In an organic solar cell, however, a donor material is used in combination with an acceptor material, so that charge recombination takes place at the donor-acceptor interface. A frequently used acceptor material is the fullerene derivative [6,6]-phenyl-C_{61}-butyric acid methyl ester (PCBM), which shows trap-free electron transport.[16] Consequently, since both hole (donor) and electron (acceptor) traps are absent in polymer:fullerene systems, electron-hole recombination between the donor and acceptor is expected to be bimolecular. However, recent studies reported on the observation of trap-assisted recombination in polymer:fullerene bulk heterojunction solar cells,[17,18] despite the virtually trap-free electron and hole transport.

To address this issue, we have studied electroluminescence (EL) from the charge-transfer state in polymer:fullerene solar cells. The charge-transfer state emission directly originates from electron-hole recombination at the donor-acceptor interface.[19] In this paper, we demonstrate that the nature of charge recombination in organic solar cells can be determined by carefully analyzing the bias-dependence of the electroluminescence and its quantum efficiency.

2. Results and Discussion

In the present study, bulk heterojunction solar cells were fabricated based on a variety of donor polymers blended with a PCBM acceptor. Among the investigated polymers are poly(3-hexylthiophene) (P3HT) and poly[2-methoxy-5-(2′-ethylhexyloxy)-*p*-phenylenevinylene] (MEH-PPV), which have served as workhorses in organic photovoltaic research.[20,21] The other two polymers used in this study are poly[9,9-didecanefluorene-*alt*-(bis-thienylene) benzothiadiazole] (PF10TBT) and poly[2,6-(4,4-bis-(2-ethylhexyl)-4*H*-cyclopenta[2,1-b;3,4-b′]-dithiophene)-*alt*-4,7-(2,1,3-benzothiadiazole)] (PCPDTBT). These are more recent wide- and narrow-bandgap polymers,

respectively, capable of giving power-conversion efficiencies between 4 and 6%.[22,23] Hence, homopolymers as well as copolymers with distinct chemical and physical properties are used, to demonstrate the generality of our approach.

2.1. Ideality Factor of Charge-Transfer State Electroluminescence

We recently demonstrated for OLEDs that the recombination mechanism, either bimolecular or trap-assisted recombination, is directly reflected in the ideality factor of the current and light output.[8] This ideality factor appears in the general Shockley diode equation, given by[24]

$$J = J_s \left[\exp\left(\frac{qV}{\eta kT} \right) - 1 \right] \qquad (1)$$

where J is the current density, J_s the (reverse bias) saturation current density, V the applied voltage, q the elementary charge, k Boltzmann's constant, T temperature, and η the ideality factor. The ideality factor equals unity in an ideal classical p-n junction diode with only direct recombination taking place. However, as shown in 1957 by a theoretical analysis of Sah, Noyce and Shockley, the presence of SRH recombination results in an enhancement of the ideality factor, reaching a value of 2 for dominant trap-assisted recombination.[25] The difference in ideality factor for bimolecular ($\eta = 1$) and trap-assisted recombination ($\eta = 2$) has recently been visualized in the different voltage dependence of the red and blue emission of white-emitting OLEDs, where both bimolecular (blue) and trap-assisted recombination (red) are emissive.[8] As a result, the ideality factor can be used as a fingerprint for the presence or absence of SRH recombination.

Ideality factors larger than unity have also been found in the dark current of polymer:fullerene solar cells, which is frequently put forward as evidence for the presence of a dominant trap-assisted recombination process.[17,18] However, we recently demonstrated that in this case the greater-than-unity ideality factor is caused by enhanced diffusion due to violation of the classical Einstein relation.[26] As a result, an ideality factor above unity can be measured even when trap-assisted recombination is completely absent.[27] The dark-current ideality factor of a polymer:fullerene bulk heterojunction solar cell therefore cannot give conclusive information about the presence or absence of trap-assisted recombination.

As described in a recent study by Tvingstedt et al.,[19] recombination at the polymer-fullerene interface is directly observable from the electroluminescence of the charge-transfer state. Charge-transfer state electroluminescence can be detected by applying a forward voltage across the solar cell and measuring the resulting emission with a silicon photodiode. Thus, the solar cell is simply operated as a light-emitting diode. As stated above, the different recombination mechanisms can directly be identified by measuring the luminance (L) ideality factor, i.e. the ideality factor of the electroluminescence intensity vs voltage characteristics. For bimolecular recombination, a luminance ideality factor of unity is expected, whereas radiative trap-assisted recombination is characterized by a luminance ideality factor of 2.

In **Figure 1**, the total electroluminescence of the investigated bulk heterojunction solar cells is plotted as a function of voltage. For all solar cells, weak luminescence could be detected, in
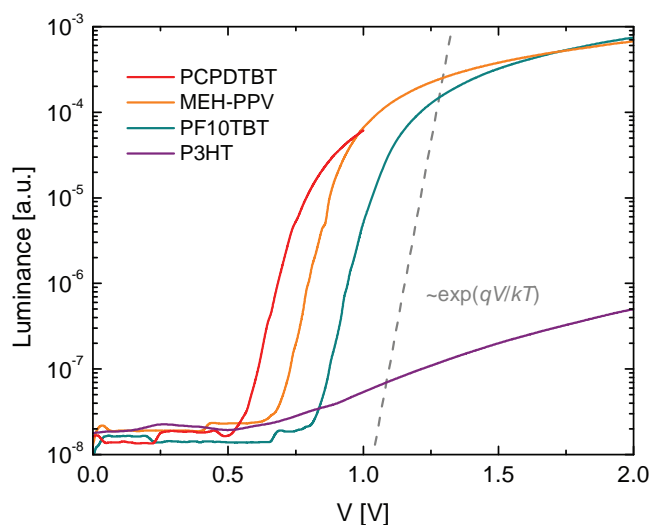

Figure 1. Luminance vs. voltage characteristics for the charge-transfer state electroluminescence of several polymer:PCBM solar cells. The onset of emission is proportional to exp(qV/kT), plotted as a dashed line as a guide to the eye.

agreement with previous studies.[19,28] At the onset of electroluminescence, the emission shows an exponential dependence on voltage according to $L \propto \exp(qV/\eta kT)$, similar to Equation 1. For the P3HT:PCBM system, the electroluminescence is too weak to resolve the exponential part of the characteristics. At higher voltages, the emission bends off from the exponential, indicating that the injected current has reached the space-charge limit. The slope of the exponential is determined by the ideality factor, which can be directly obtained by numerical differentiation according to

$$\eta = \left(\frac{kT}{q} \frac{\partial \ln L}{\partial V} \right)^{-1} \qquad (2)$$

This derivative is plotted as a function of voltage in **Figure 2**, where the ideality factor can be obtained from the minimum
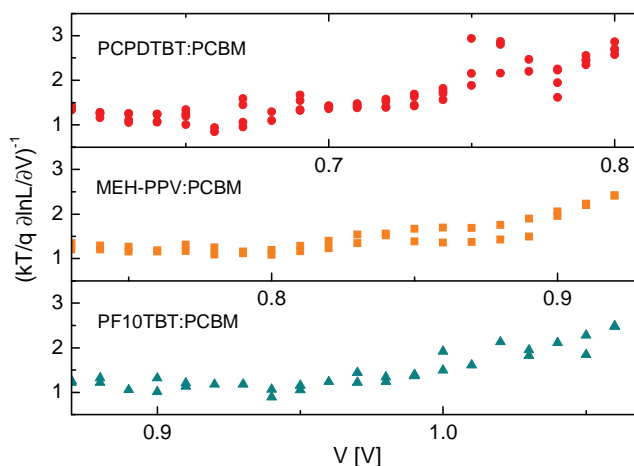

Figure 2. Luminance ideality factor of the charge-transfer state electroluminescence of the investigated polymer:PCBM solar cells, obtained by numerical differentiation according to Equation 2. For all three systems the curves approach unity at low voltages, indicative of a luminance ideality factor of 1.

ADVANCED
ENERGY
MATERIALS
www.advenergymat.de

Materials
Views
www.MaterialsViews.com

or plateau value of the characteristics.[8] Note that it is difficult to obtain a long plateau value due to weak electroluminescence and a limited sensitivity of the photodiode. It is clear from Figure 2 that the ideality factor approaches unity for the investigated solar cells. The ideality factor of 1 reveals that charge-transfer state emission originates from a free-carrier, bimolecular recombination process. From these measurements, we can thus exclude the presence of radiative trap-assisted recombination. This is in agreement with the measurements on very similar systems by Tvingstedt et al.,[19] where no additional low-energy feature could be observed from the CT-state electroluminescence spectra.

2.2. Charge-Transfer State Electroluminescence Efficiency

Clearly, electroluminescence from the charge-transfer state can shed light on the radiative recombination routes. However, the nonradiative part of the recombination process cannot be identified directly in this way. As recombination via trap states is usually nonradiative,[8] a definitive statement about its absence or presence cannot be made. In a recent study,[8] it has been shown that trap-assisted recombination has a weaker voltage dependence than bimolecular recombination, since the former has a linear charge-density dependence and the latter a quadratic density dependence. As a result, radiative bimolecular recombination becomes more important than the competing nonradiative trap-assisted recombination with increasing bias voltage.[8–10] The direct consequence is that the

conversion efficiency of electrical charge carriers into photons increases also with voltage, in the case that both mechanisms are present.[9] When only either of the two recombination channels is present, the quantum efficiency of luminescence is expected to be voltage independent. The reason is that, although the recombination rate itself is density- and hence voltage-dependent, recombination is present in the luminescence as well as in the current. The EL efficiency is the ratio between the luminescence and the current. If luminescence and current are governed by the same recombination mechanism, their voltage (density) dependence is cancelled when calculating the efficiency, resulting in a voltage-independent EL efficiency. However, when the radiative bimolecular recombination (second order) is accompanied by a nonradiative trap-assisted recombination (first order) process, the EL efficiency will increase with voltage.

Therefore, we plotted the EL quantum efficiency, calculated by dividing the photodiode signal by the injection current of the solar cell, as a function of voltage in **Figure 3**. For solar cells made from PCPDTBT, MEH-PPV and PF10TBT, the luminous efficiency is voltage independent. Since it has been verified that the charge-transfer state emission originates from bimolecular free-carrier recombination, the voltage-independent efficiency proves the absence of a competing nonradiative recombination process of trap-assisted nature. For the P3HT:PCBM system however, a clearly different trend is observed. The efficiency increases with voltage, characteristic of the presence of a nonradiative trap-assisted recombination mechanism competing with radiative bimolecular recombination.[9]
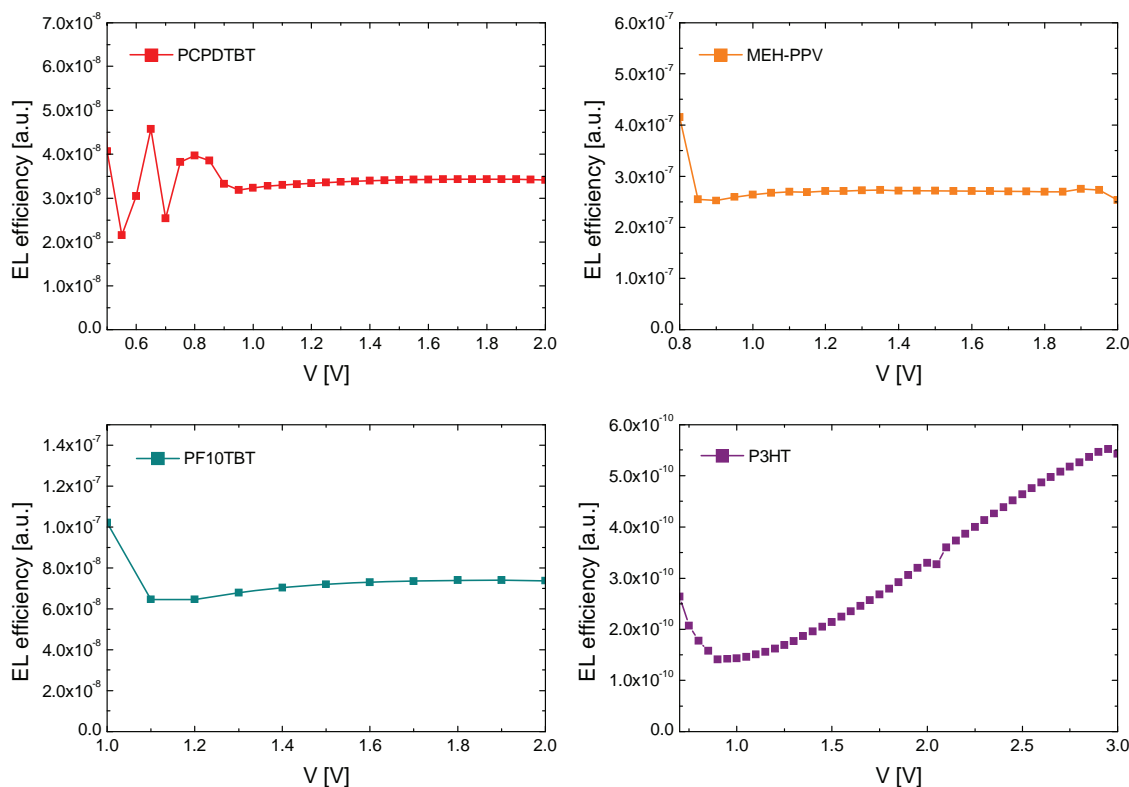

Figure 3. Electroluminescence quantum efficiency of the charge-transfer state emission as a function of the applied voltage. Except for P3HT:PCBM, the EL efficiency is virtually voltage independent.

www.MaterialsViews.com

ADVANCED
ENERGY
MATERIALS
www.advenergymat.de

FULL PAPER

The observation of dominant bimolecular recombination in PCPDTBT, MEH-PPV and PF10TBT solar cells is in agreement with our recent study where we measured the light-intensity (I) dependence of the open-circuit voltage (V_{oc}) of these systems.[26] It is well established that SRH-type trap-assisted recombination causes an increased slope of V_{oc} vs ln(I), which has a value of kT/q when trap-assisted recombination is absent.[6,7] A slope of kT/q was measured for PCPDTBT, MEH-PPV and PF10TBT solar cells, arising from dominant bimolecular free-carrier recombination. This is confirmed by our measurements of the charge-transfer state luminescence ($\eta = 1$) and its voltage-independent efficiency. Interestingly, P3HT:PCBM solar cells showed a voltage-dependent efficiency of the luminescence of the charge-transfer state, indicative of an additional trap-assisted recombination process being present. Consequently, these solar cells should also exhibit an enhanced light-intensity dependence of the open-circuit voltage. This is indeed what we observe in **Figure 4**. In contrast to the other investigated systems, the P3HT-based solar cell shows a slope of V_{oc} vs ln(I) that is significantly larger than kT/q, implying the presence of a lower-order recombination mechanism. The slope of 1.25 kT/q is in agreement with previously obtained values[29] and once more confirms the interpretation of the voltage-dependent EL efficiency. It should be noted that similar slopes were obtained using P3HT obtained from different sources (see Experimental Section) and processing the films from different solvents.

The qualitative agreement of the EL ideality factor and efficiency measurements with the intensity dependence of V_{oc} shows that our electroluminescence measurements are a relevant representation of recombination mechanisms in organic solar cells under operating conditions. Important in the comparison between recombination of photogenerated and voltage-generated charges is the electric-field and charge-density regime in which the measurements are performed. The ideality factor
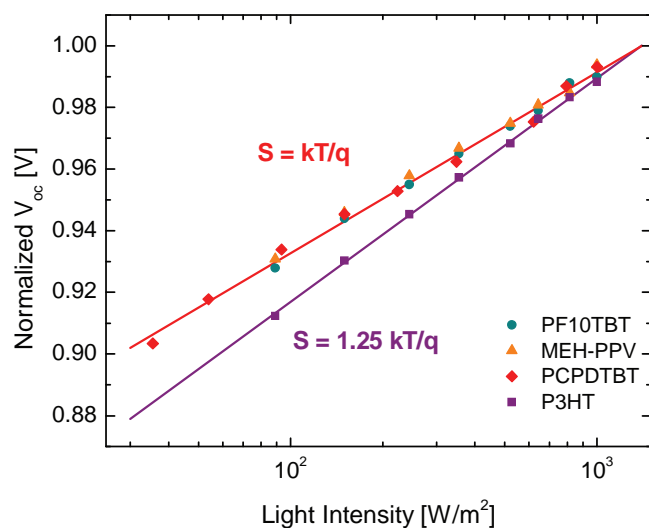
of the CT-state electroluminescence is obtained in the voltage regime just below the open-circuit voltage, which is actually close to the voltage of the maximum-power point. As the measurements are performed near flat-band conditions and in dark, the charge density in the EL ideality factor experiment is lower than under illumination. Since trap-assisted recombination (if present) is more dominant at lower densities,[8,9] the amount of trap-assisted recombination is expected to be even lower under illumination.

The EL efficiency measurements are performed in a regime where the effective applied electric field is similar to the fields in solar cells under operating conditions (although in opposite direction). As charge density is increased with applied voltage, a crossover from trap-assisted (if present) to bimolecular recombination is expected to occur in a certain voltage range, which is observed only for P3HT.

2.3. Trap-Assisted Recombination in P3HT:PCBM

Although both independent EL and V_{oc} measurements indicate a substantial influence of an SRH-type recombination channel in P3HT:PCBM, the occurrence of this mechanism is not straightforward. The appearance of trap-assisted recombination requires the presence of a density of trap states, which should give rise to the observation of trap-limited charge transport. However, the transport characteristics as measured in single-carrier diodes of P3HT and PCBM show trap-free behavior, which contradicts the presence of a large trap density.

This apparent discrepancy can be resolved by considering the fact that recombination of free and trapped carriers are competing processes. As a consequence, the observation of an SRH mechanism can also be due to a reduced bimolecular recombination rate. Bimolecular recombination in organic semiconductors is usually of the Langevin type, for which the recombination coefficient is given by[3]

$$k_L = \frac{q}{\varepsilon}(\mu_n + \mu_p) \qquad (3)$$

with ε the dielectric constant and μ_n and μ_p the electron and hole mobility, respectively. For P3HT:PCBM solar cells however, reduced bimolecular recombination rates were measured.[30–32] The experimentally obtained value for the bimolecular recombination coefficient in those cells is approximately a factor 1000 lower than for conventional Langevin recombination.

Since the bimolecular Langevin recombination rate is greatly reduced in the P3HT:PCBM system, it is expected that SRH recombination can become apparent even when the trap density is small. To investigate at which trap density the transport is affected such that it can be observed experimentally, numerical drift-diffusion simulations[33] were carried out. **Figure 5** shows simulations of the J–V characteristics of a P3HT hole-only diode for increasing hole-trap densities. It is clear that the effect of charge trapping on the hole current becomes negligible at trap densities below 2×10^{21} m^{-3}, and hence impossible to observe from experimental J–V characteristics.

The next step is to investigate whether such low trap densities are sufficient to explain the light-intensity dependence of V_{oc} when a reduced bimolecular recombination rate is taken

Figure 4. Normalized V_{oc} vs incident light intensity for the investigated polymer:fullerene solar cells. For P3HT:PCBM, the best fit to the data (solid line) has a slope (S) of 1.25 kT/q. The other investigated cells are well described by a line with a slope of kT/q. The V_{oc} was normalized by addition of a constant so that the best fits of the separate datasets coincide at an intensity of 1400 W/m^2.
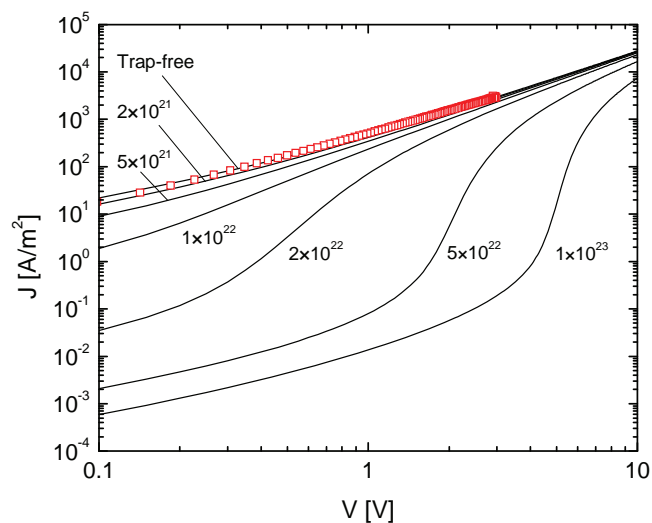
Figure 5. Experimental (symbols) and simulated (lines) J–V characteristics of a P3HT hole-only device. The simulations are performed for increasing hole-trap densities [m^{-3}] of a single-level trap with a depth of 0.5 eV.

into account. Therefore, current-voltage characteristics of a P3HT:PCBM solar cell were simulated, where the competing recombination mechanisms were introduced in the simulations as described in reference [8]. A trap density of 2×10^{21} m^{-3} was already sufficient to described the enhanced V_{oc} vs light intensity dependence of P3HT:PCBM. (**Figure 6**), assuming that the bimolecular recombination rate was reduced by a factor 1000 as compared to the Langevin formula, in turn increasing the
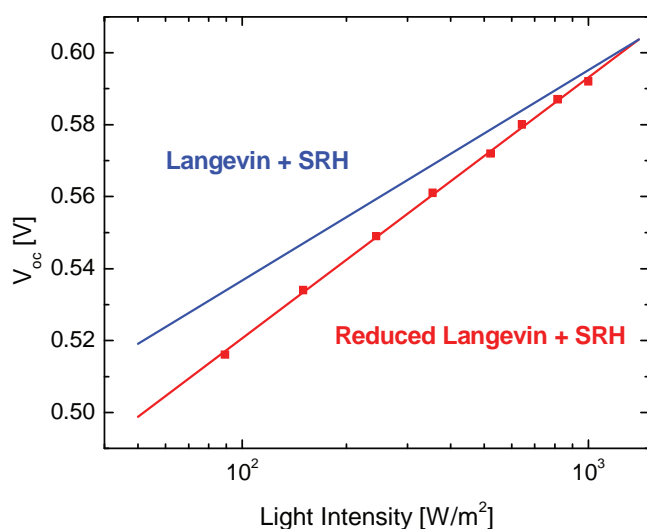

Figure 6. V_{oc} vs incident light intensity for a P3HT:PCBM solar cell (symbols). The lines represent simulations of a drift-diffusion model assuming a trap concentration of 2×10^{21} m^{-3} and are normalized at $I = 1400$ W/m^2. A slope of kT/q was found when using the Langevin formula for bimolecular recombination, whereas an enhanced slope was found when a reduced bimolecular recombination rate was introduced, in agreement with the experimental data.

relative SRH contribution. Similar low trap concentrations have been measured for P3HT in recent studies.[34–38] As is obvious from Figure 5, such a low trap density cannot be observed experimentally from the current of a single-carrier diode, so that the charge transport appears to be trap free. It should be noted that a slope of kT/q was obtained for the V_{oc}-ln(I) data when bimolecular recombination would follow the conventional Langevin expression.

3. Conclusion

In conclusion, it was demonstrated that the nature of charge recombination in organic solar cells can be identified from the charge-transfer state electroluminescence. By measuring the slope of the onset of electroluminescence as a function of voltage, it was demonstrated that radiative recombination at the donor-acceptor interface originates from a bimolecular process. Nonradiative recombination becomes apparent when measuring the efficiency of the conversion of electrical charges into photons. The presence of nonradiative trap-assisted recombination gives rise to an increase in EL efficiency as a function of bias. Such voltage-enhanced efficiency was observed only for P3HT:PCBM, whereas the other investigated systems showed a voltage-independent EL efficiency. Hence, P3HT:PCBM comprises an additional trap-assisted recombination channel, whereas bimolecular free-carrier recombination is dominant in the other solar cells. Ultimately, this was confirmed by measurements on the light intensity-dependence of the open-circuit voltage. The manifestation of SRH-type trap-assisted recombination in P3HT:PCBM bulk heterojunction solar cells is attributed to a reduced competing bimolecular recombination rate. In that case, a small number of trapping sites is sufficient to cause an enhanced light-intensity dependence of V_{oc}, while having only a minor effect on charge transport.

4. Experimental Section

Device Fabrication: For the fabrication of the polymer:fullerene solar cells, glass substrates, prepatterned with indium tin oxide, were thoroughly cleaned by washing with detergent solution and ultrasonication in acetone and isopropyl alcohol, followed by UV-ozone treatment. The cleaned substrates were coated in ambient air with a 60 nm thick film of poly(3,4-ethylenedioxythiophene):poly(styrenesulfonic acid) (VP AI4083, H.C. Starck). Subsequently, photoactive layers with a thickness of 80–100 nm of PCPDTBT:PCBM (1:2), MEH-PPV:PCBM (1:4), PF10TBT:PCBM (1:4) and P3HT:PCBM (1:1) were deposited by spin coating from chlorobenzene solution under N$_2$ atmosphere. The P3HT:PCBM layers were annealed in N$_2$ atmosphere for 10 min at 140 °C, immediately after deposition. The devices were finished by thermal evaporation of a LiF(1 nm)/Al(100 nm) cathode at a base pressure of 1×10^{-6} mbar. Hole-only devices were fabricated similarly in a glass/ITO/PEDOT:PSS/P3HT/Au structure. P3HT was obtained from Rieke Metals, Inc. (4002-EE) and Plextronics, Inc. (Plexcore OS 2100).

Device Characterization: Electrical measurements were conducted under controlled N$_2$ atmosphere, using a computer-controlled Keithley 2400 source meter. Electroluminescence was recorded simultaneously using a Hamamatsu S1336 silicon photodiode. For the measurements under illumination, a Steuernagel SolarConstant 1200 metal halide lamp was used, which was set to 1 sun intensity using a silicon reference cell and correcting for spectral mismatch. Intensity-dependent

measurements were performed by using a set of neutral-density filters to decrease the illumination level.

[1] M. A. Green, K. Emery, Y. Hishikawa, W. Warta, E. D. Dunlop, *Prog. Photovoltaics Res. Appl.* **2012**, *20*, 12.

[2] R. F. Service, *Science* **2011**, *332*, 293.

[3] P. Langevin, *Ann. Chim. Phys.* **1903**, *28*, 433.

[4] P. W. M. Blom, M. J. M. de Jong, S. Breedijk, *Appl. Phys. Lett.* **1997**, *71*, 930.

[5] A. Pivrikas, G. Juška, R. Österbacka, M. Westerling, M. Viliūnas, K. Arlauska, H. Stubb, *Phys. Rev. B* **2005**, *71*, 125205.

[6] M. M. Mandoc, F. B. Kooistra, J. C. Hummelen, B. de Boer, P. W. M. Blom, *Appl. Phys. Lett.* **2007**, *91*, 263505.

[7] M. M. Mandoc, W. Veurman, L. J. A. Koster, B. de Boer, P. W. M. Blom, *Adv. Funct. Mater.* **2007**, *17*, 2167.

[8] G. A. H. Wetzelaer, M. Kuik, H. T. Nicolai, P. W. M. Blom, *Phys. Rev. B* **2011**, *83*, 165204.

[9] M. Kuik, H. T. Nicolai, M. Lenes, G. A. H. Wetzelaer, M. Lu, P. W. M. Blom, *Appl. Phys. Lett.* **2011**, *98*, 093301.

[10] M. Kuik, L. J. A. Koster, G. A. H. Wetzelaer, P. W. M. Blom, *Phys. Rev. Lett.* **2011**, *107*, 256805.

[11] S. R. Cowan, W. L. Leong, N. Banerji, G. Dennler, A. J. Heeger, *Adv. Funct. Mater.* **2011**, *21*, 3083.

[12] W. Shockley, W. T. Read, *Phys. Rev.* **1952**, *87*, 835.

[13] a) R. N. Hall, *Phys. Rev.* **1951**, *83*, 228; b) R. N. Hall, *Phys. Rev.* **1952**, *87*, 387.

[14] P. W. M. Blom, M. J. M. de Jong, J. J. M. Vleggaar, *Appl. Phys. Lett.* **1996**, *68*, 3308.

[15] M. M. Mandoc, B. de Boer, G. Paasch, P. W. M. Blom, *Phys. Rev. B* **2007**, *75*, 193202.

[16] V. D. Mihailetchi, J. K. J. van Duren, P. W. M. Blom, J. C. Hummelen, R. A. J. Janssen, J. M. Kroon, M. T. Rispens, W. J. H. Verhees, M. M. Wienk, *Adv. Funct. Mater.* **2003**, *13*, 43.

[17] R. A. Street, M. Schoendorf, A. Roy, J. H. Lee, *Phys. Rev. B* **2010**, *81*, 205307.

[18] T. Kirchartz, B. E. Pieters, J. Kirkpatrick, U. Rau, J. Nelson, *Phys. Rev. B* **2011**, *83*, 115209.

[19] K. Tvingstedt, K. Vandewal, A. Gadisa, F. Zhang, J. Manca, O. Inganas, *J. Am. Chem. Soc.* **2009**, *131*, 11819.

[20] G. Yu, J. Gao, J. C. Hummelen, F. Wudl, A. J. Heeger, *Science* **1995**, *270*, 1789.

[21] F. Padinger, R. S. Ritterberger, N. S. Sariciftci, *Adv. Funct. Mater.* **2003**, *13*, 85.

[22] L. H. Slooff, S. C. Veenstra, J. M. Kroon, D. J. D. Moet, J. Sweelssen, M. M. Koetse, *Appl. Phys. Lett.* **2007**, *90*, 143506.

[23] J. Peet, J. Y. Kim, N. E. Coates, W. L. Ma, D. Moses, A. J. Heeger, G. C. Bazan, *Nat. Mater.* **2007**, *6*, 497.

[24] W. Shockley, *Bell Syst. Tech. J.* **1949**, *28*, 435.

[25] C. T. Sah, R. N. Noyce, W. Shockley, *Proc. IRE* **1957**, *45*, 1228.

[26] G. A. H. Wetzelaer, M. Kuik, M. Lenes, P. W. M. Blom, *Appl. Phys. Lett.* **2011**, *99*, 153506.

[27] G. A. H. Wetzelaer, L. J. A. Koster, P. W. M. Blom, *Phys. Rev. Lett.* **2011**, *107*, 066605.

[28] K. Vandewal, K. Tvingstedt, A. Gadisa, O. Inganäs, J. V. Manca, *Nat. Mater.* **2009**, *8*, 904.

[29] M. Lenes, S. W. Shelton, A. B. Sieval, D. F. Kronholm, J. C. Hummelen, P. W. M. Blom, *Adv. Funct. Mater.* **2009**, *19*, 3002.

[30] A. Pivrikas, G. Juška, A. J. Mozer, M. Scharber, K. Arlauskas, N. S. Sariciftci, H. Stubb, R. Österbacka, *Phys. Rev. Lett.* **2005**, *94*, 176806.

[31] G. Juška, K. Arlauskas, J. Stuchlik, R. Österbacka, *J. Non-Cryst. Solids* **2006**, *352*, 1167.

[32] C. Deibel, A. Baumann, V. Dyakonov, *Appl. Phys. Lett.* **2008**, *93*, 163303.

[33] L. J. A. Koster, E. C. P. Smits, V. D. Mihailetchi, P. W. M. Blom, *Phys. Rev. B* **2005**, *72*, 085205.

[34] J. Schafferhans, A. Baumann, C. Deibel, V. Dyakonov, *Appl. Phys. Lett.* **2008**, *93*, 093303.

[35] G. Garcia-Belmonte, P. P. Boix, J. Bisquert, M. Sessolo, H. J. Bolink, *Sol. Energy Mater. Sol. Cells* **2010**, *94*, 366.

[36] K. S. Nalwa, R. C. Mahadevapuram, S. Chaudhary, *Appl. Phys. Lett.* **2011**, *98*, 093306.

[37] S. Khelifi, K. Decock, J. Lauwaert, H. Vrielinck, D. Spoltore, F. Piersimoni, J. Manca, A. Belghachi, M. Burgelman, *J. Appl. Phys.* **2011**, *110*, 094509.

[38] P. P. Boix, J. Ajuria, I. Etxebarria, R. Pacios, G. Garcia-Belmonte, *Thin Solid Films* **2012**, *520*, 2265.